



Influence of H₂O on NO formation during char oxidation of biomass

Karlström, Oskar; Wu, Hao; Glarborg, Peter

Published in:
Fuel

Link to article, DOI:
[10.1016/j.fuel.2018.08.156](https://doi.org/10.1016/j.fuel.2018.08.156)

Publication date:
2019

Document Version
Peer reviewed version

[Link back to DTU Orbit](#)

Citation (APA):
Karlström, O., Wu, H., & Glarborg, P. (2019). Influence of H₂O on NO formation during char oxidation of biomass. *Fuel*, 235, 1260-1265. <https://doi.org/10.1016/j.fuel.2018.08.156>

General rights

Copyright and moral rights for the publications made accessible in the public portal are retained by the authors and/or other copyright owners and it is a condition of accessing publications that users recognise and abide by the legal requirements associated with these rights.

- Users may download and print one copy of any publication from the public portal for the purpose of private study or research.
- You may not further distribute the material or use it for any profit-making activity or commercial gain
- You may freely distribute the URL identifying the publication in the public portal

If you believe that this document breaches copyright please contact us providing details, and we will remove access to the work immediately and investigate your claim.

1 Influence of H₂O on NO formation during char oxidation of biomass

2 Oskar Karlström^{*a}, Hao Wu^b, Peter Glarborg^b

3 ^aJohan Gadolin Process Chemistry Centre, Åbo Akademi University, Finland

4 ^bDepartment of Chemical and Biochemical Engineering, Technical University of Denmark

5 ^{*}corresponding author, email: okarlstr@abo.fi, address: Piispankatu 8 20500 Turku, Finland

6 Abstract

7 The present study investigates conversion of char-N to NO in mixtures of O₂/N₂ and in O₂/H₂O/N₂.
8 Biomass particles of spruce bark were combusted in an electrically heated single particle reactor at
9 900 °C at various O₂/H₂O/N₂ concentrations. NO concentrations of the product gases were measured
10 during the char combustion stage. The conversion of char-N to NO was significantly higher with H₂O as
11 compared to without H₂O in the gas. Additional fixed bed experiments were conducted to investigate
12 the products of the reaction between H₂O and spruce bark char. The results showed that NH₃ is the
13 primary product in the reaction between char-N and steam. These results explain the observation that
14 more NO is formed during char combustion in the presence of steam: the char-N reacts partly with
15 H₂O to form NH₃, which reacts further to NO.

16 **Keywords:** biomass; char; NO; NH₃, gasification, steam gasification, combustion, oxidation

17 1. Introduction

18 Combustion and gasification of biomass generate NO_x emissions. In combustion and gasification of
19 biomass most of the NO_x origins from the fuel bound nitrogen (fuel-N) [1]. Some biomasses such as
20 pine or birch wood have relatively low nitrogen contents [2] while for example algae or many
21 agricultural biomasses have relatively high nitrogen contents [3]. However, because of very strict NO
22 legislations and environmental reasons, even biomasses with low N contents may give rise to too high
23 NO_x emissions, requiring expensive cleaning strategies [4]. Around 70-90% of the fuel-N is bound to

24 the volatile matter (vol-N) and released during devolatilization [2]. The remaining part, around 10-30%,
25 is mostly bound to the char (char-N) [3]. For some biomasses, such as black liquor, the split differs: for
26 black liquor the char-N may account for more than 50% of the fuel-N [5]. During devolatilization, the
27 vol-N reacts to NH_3 , HCN, HNCN, NO, N_2O , N_2 and tar-N [6]. The product distribution depends on the
28 nitrogen content of the fuel, volatile matter, heating rate, final temperature, surrounding gas
29 atmosphere, and how the nitrogen is bound to the fuel [1]. During char conversion, char-N reacts with
30 O_2 to NO. The NO formed from the char-N does not, however, correspond to the release of NO from
31 the same char particle, since it can be reduced to N_2 within the pore system [7,8]. Interestingly, the
32 conversion of char-N to NO increases with decreasing particle size [7–10]. This can be explained by the
33 fact that for a small particle more of the initially formed NO diffuse out from the particle resulting in
34 less possibility for intra-particle reduction of NO to N_2 [11]. For coal chars the influence of steam and
35 CO_2 on char-N conversion has been investigated. Park et al. [12] suggested that coal char-N reacts with
36 CO_2 forming N_2 , while char-N reacts with H_2O forming NH_3 , HCN and N_2 . As NH_3 and HCN are NOx
37 precursors [1,13,14], the NOx emissions vary dependent on whether the combustion occurs in O_2/N_2
38 or in $\text{O}_2/\text{CO}_2/\text{H}_2\text{O}/\text{N}_2$. In combustion and gasification, the char conversion always occurs in an
39 environment with H_2O and CO_2 present, besides O_2 [15–17].

40 The present study investigates conversion of biomass char-N to NO in O_2/N_2 and in $\text{O}_2/\text{H}_2\text{O}/\text{N}_2$ in a
41 single particle reactor. The biomass which is investigated is spruce bark char. Barks often have
42 relatively high nitrogen contents in comparison to many other biomass fuels. Bark is one of the main
43 residues from the wood and paper industry and is one of the most significant biomasses used in
44 industrial thermal conversion. In addition, fixed bed reactor experiments are performed between H_2O
45 and the bark char in order to quantify the release of NH_3 under steam gasification conditions.

46

47 **2. Experiments**

48 Experiments were conducted in a single particle reactor (section 2.2) and in a fixed bed reactor (section
 49 2.3). For the single particle reactor experiments, pellets were pressed from spruce bark particles, while
 50 in the fixed bed reactor char produced from the spruce bark was used.

51 **2.1 Materials**

52 Samples of spruce bark were ground and sieved to a size fraction of 250–1000 μm . Single particle
 53 samples were prepared by pressing 200 mg of parent biomass into cylindrical pellets with a diameter
 54 of 8 mm. A single pellet is hereafter referred to as a single particle. The carbon, hydrogen, nitrogen,
 55 and sulfur contents of the samples and of the chars were analyzed with a Thermo Scientific Flash 2000
 56 Organic Element Analyzer (Flash 2000) (see Table 1). Chars for elemental analysis were produced by
 57 inserting the parent fuel in N_2 and removing the chars after the devolatilization had ended. In the NO
 58 release experiments the chars were produced in situ. The metal content of the biomass samples were
 59 analyzed by inductively coupled plasma optical emission spectroscopy (ICP-OES) (see Table 2).

60 Table 1. CNHS of fuel and char.

	wt-% on dry basis					char yield (%)	Ash content (%)
	N	C	H	S	O*		
spruce bark	0.27	46.2	5.8	0.00	43.3	24.9	4.4
spruce bark char	0.32	74.5	0.99	0.00	6.5	100.0	17.7

61 *by difference

62 Table 2. Elemental analysis of fuel and char.

	mg/kg (db)											
	Al	Ca	Fe	K	Mg	Mn	Na	P	S	Si	Ti	Zn
spruce bark	206	11499	140	1496	684	610	< 120	297	241	283	5	45
spruce bark char	676	36142	510	4995	2237	1981	< 120	929	278	697	15	< 4

63

64

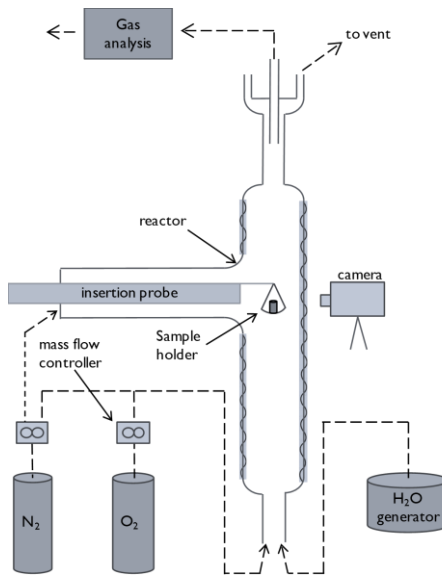


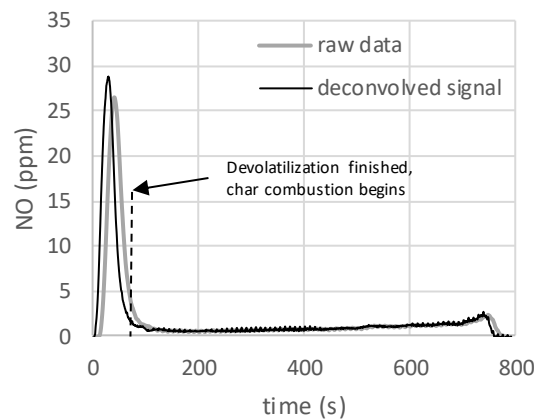
Fig. 1. Single particle reactor for combustion experiments [18].

2.2 Single particle reactor

Experiments were conducted in a single particle reactor at 900 °C in the following gas mixtures with N₂ as the balance gas (% refers here to vol.%): 1% O₂ /14%H₂O, 3% O₂ /14%H₂O, 6% O₂ /14%H₂O, 3% O₂, 6% O₂ and 9% O₂. Chars were produced by inserting the parent fuel in N₂ and removing the chars after the devolatilization had ended.

A detailed description of the reactor can be found elsewhere [18,19]. The single particle reactor consists of a quartz tube reactor inserted in a ceramic furnace. The inner diameter of the tube is 44.3 mm. Gas mixtures of oxygen, nitrogen and steam were fed in the bottom of the reactor and the product gases left from the top of the reactor. Nitrogen was also injected from three sides of the reactor system, on the same level as the particle insertion, to ensure a good mixing of the gases. The biomass sample was inserted into the reactor using a movable horizontal probe that could be inserted from room temperature into the hot reactor within one to two seconds. The sample holder consisted of a thin net on which a single fuel pellet was placed. Concentrations of NO, CO₂ and CO in the outlet gases were continuously measured with a Teledyne Instruments Model 200E and with an ABB AO2020 analyzer. The measuring ranges of the CO and CO₂ analyzers are 0-10%, and the measuring range for

82 the NO_x analyzer is 0-60 ppm. The accuracy of the CO and CO₂ analyzers is 0.01%, while the accuracy
83 of the NO analyzer is 0.1 ppm. The measurement accuracies of the analyzers are those as reported by
84 the analyzer manufacturers. Figure 2 shows raw data from a test with 3% O₂. Because of the residence
85 time distribution of the reactor system, the release of N, according to the measured NO signal, differs
86 from the release of N from the particle. For this reason, the measured signal was deconvolved using
87 the residence time distribution based on a step response test. Figure 2 shows two distinct behaviors:
88 (1) the first peak occurring during the first 60 seconds representing the devolatilization and (2) the
89 slower char oxidation stage. In the present study, only the char oxidation stage is considered. All
90 experiments were repeated at least two times and the repeatability was good (repetitions shown in
91 supplementary material).



92

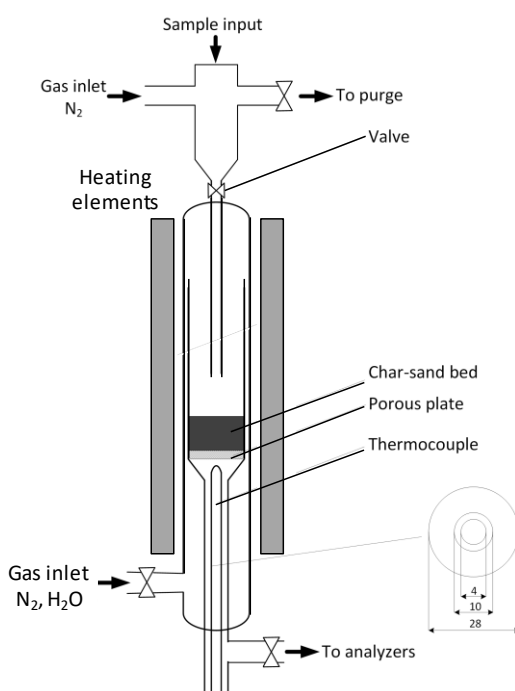
93 Fig. 2. NO ppm raw data from single particle reactor and deconvolved signal at 900 °C and with 3% O₂
94 in the gas.

95

96 2.3 Fixed bed reactor

97 Figure 3 shows the quartz fixed bed reactor used for NH₃ measurements from steam gasification
98 experiments. The reactor is similar to that employed by Zhao et al [20]. Three independent heating
99 elements ensured a uniform temperature gradient. A thermocouple, located 0.5 cm below the porous
100 plate on which the gasification reactions took place, measured the reaction temperature. A solid
101 feeding device allowed the admission of samples at the desired temperature and gas phase

102 composition in the reactor. In the experiments, 2 g of quartz sand with a size of 250-355 μm , treated
 103 at 800°C, was added together with 100 mg of char samples to ensure plug flow through the bed and
 104 facilitate the sample admission. The chars for the fixed bed experiments were produced at 900 °C in
 105 100% N_2 . Blank tests revealed that the treated sand resulted in no release of NH_3 . The experiments
 106 were conducted at 900 °C with 3% steam in the gas. NH_3 concentrations of product gases were
 107 continuously measured with an ABB AO2020 Analyzer (Limas11 HW). The measuring range for the NH_3
 108 analyzer is 0-1000 ppm. The accuracy of the NH_3 analyzer < 2% of the measurement range.



109

110 Fig. 3. Fixed bed reactor for steam gasification and NH_3 measurements [20].

111 **2.4 Split of N in char and volatiles**

112 The N contents of the parent fuel and char were 0.27 and 0.32 wt.%, respectively. The N content of
 113 the char was 0.08 wt.% on initial fuel basis (0.32 wt.% x 0.249) and the N content of the volatile matter
 114 was 0.19 wt.% on initial fuel basis. Thus, the split vol-N/char-N was 70%/30%.

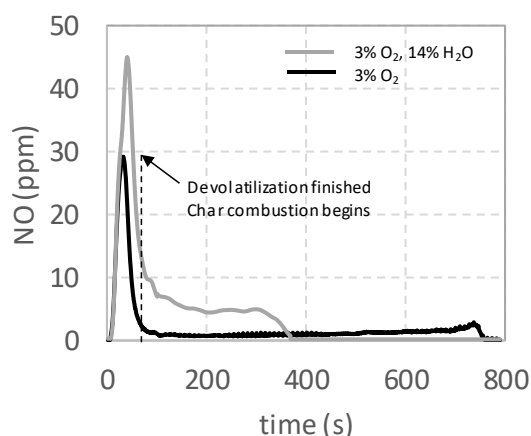
115

116

117 **3. Results and Discussion**

118 **3.1 Conversion of char-N to NO**

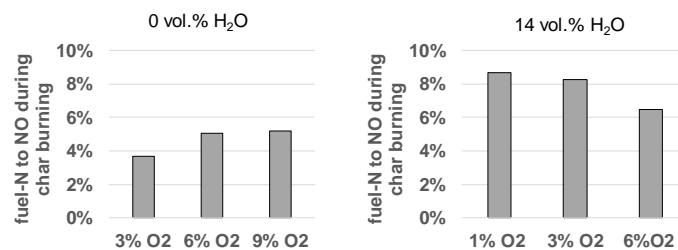
119 Figure 4 shows experimental NO concentrations during the combustion in 3 % O₂ and in 3% O₂/14%
120 H₂O. The char conversion occurs more rapidly in 3% O₂/14% H₂O than in 3% O₂. This can be explained
121 by the rapid char gasification rates in the presence of H₂O. Single particle tests were also done without
122 O₂ and with 14% H₂O. In these tests NO was not observed during the char gasification. The total
123 conversion time (not shown here), including devolatilization, based on measured CO and CO₂
124 concentrations was around 500 seconds in 0% O₂/14% H₂O, as compared to 370 seconds in 3% O₂/14%
125 H₂O, and 750 seconds in 3% O₂/0% H₂O. The rapid carbon conversion rates in steam can be explained
126 by the presence of catalytic elements, i.e., K and Ca (see table 2) [21,22].



127
128 Fig. 4. NO versus time in O₂ and in O₂/H₂O from a single particle combustion tests of spruce bark at
129 900 °C.

130
131 The NO levels during the char conversion stage are significantly higher when steam is present in the
132 gas. To determine the amounts of nitrogen released as NO during the char conversion, the measured
133 curves were integrated and recalculated to amounts of nitrogen based on the total flow through the
134 reactor. In Fig. 4, around 15% of the char-N formed NO in the case without steam, while almost 30%
135 of the char-N formed NO in the case with steam. Figure 5 shows the amounts of N released as NO for
136 the six different cases. In all cases, the amounts of N released as NO are significantly higher with steam

137 present in the gas. To the authors' knowledge, the influence of steam on the NO release has not been
 138 observed previously. Different trends regarding the conversion of fuel-N to NO may be observed in the
 139 cases with and without steam in the gas. In the case without steam, the conversion of char-N to NO
 140 increases with increased O₂ concentration, while in the case with steam, the conversion of char-N to
 141 NO decreases with increased O₂ concentration. In the different cases, 3-8 % of the initial fuel-N (around
 142 10-30% of the char-N) is released as NO during the char combustion stage. The conversion of char-N
 143 to NO has been found to be lower, in general, than 50% in environments of O₂/N₂ [2,9,10,18,19,23]. In
 144 a few cases conversions of char-N to NO as high as 70% have been reported [10,19].



145
 146 Fig. 5. Amounts of N released as NO during char combustion from single spruce bark pellets at 900 °C
 147 with and without H₂O in the gas.

148 In Fig. 4, the shapes of the NO release curves differ during the char combustion stage. In O₂/N₂, the NO
 149 release increases throughout the char conversion. This has been observed in previous studies and can
 150 be explained by the fact that as the char is consumed and the char particle decreases in size, there is
 151 less possibility for initially formed NO to be reduced to N₂ [7-11]. This interesting trend cannot be
 152 observed for the char conversion in O₂/H₂O/N₂. One explanation for this is that the char-N is not initially
 153 forming NO, but instead an NO precursor, so that the heterogeneous NO reduction step is eliminated.

154 3.2 Influence of H₂O and O₂ on char conversion

155 The oxidation of carbon and nitrogen has been assumed to be non-selective for coal chars [7,8,24,25],
 156 with some exceptions [26,27]. The relative contributions of H₂O, O₂ and CO₂ on the conversion of
 157 biomass char-N have not been investigated. This is a difficult task, as the reactions of char-N are side
 158 reactions: the main reactions are the ones with char-C. In fact, the relative contributions of H₂O, O₂

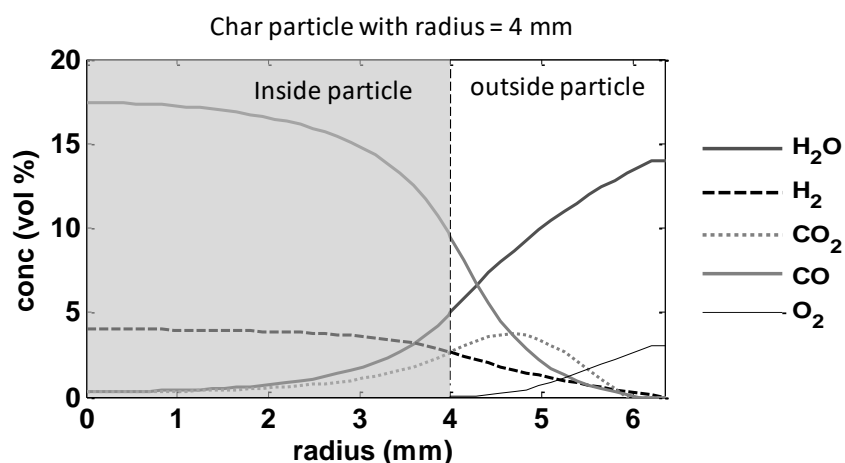
159 and CO₂ on char-C conversion in biomass combustion has not been investigated in detail. At
160 sufficiently low temperatures, O₂ is the primary gaseous reactant, but as the temperature increases,
161 also CO₂ and H₂O oxidize the char-C. For coal chars, H₂O and CO₂ play an important role in oxidizing the
162 carbon at very high temperatures such as in pulverized fuel combustion. Stanmore and Visona [28]
163 showed that, for pulverized coal char particles, H₂O and CO₂ can contribute to char conversion already
164 at 1200 °C. Based on Fig. 4, it is obvious that steam strongly contributes to the conversion of the
165 investigated biomass char at 900 °C.

166 In order to determine the relative contributions of H₂O and O₂ a detailed single particle model was
167 used [29]. The model equations and assumptions for the modeling are available in the supplementary
168 material. The single particle model takes into consideration homogeneous chemistry and temperature
169 gradients in the boundary layer of the particle. The reactions between O₂ and char-C are assumed mass
170 transfer limited. Kinetic parameters for steam gasification reactions were determined by fitting
171 computed char gasification times to experimentally determined char gasification times at 900 °C in
172 H₂O/N₂.

173 Figure 6 shows computed concentrations of the main gaseous species inside the particle and in the
174 boundary layer of the particle combusted in 3% O₂/14% H₂O. These computations were done to
175 investigate the contribution of steam gasification in the single particle reactor experiments. The same
176 particle size, i.e. 8 mm, is used as in the experiments. It can be seen that little O₂ reaches the particle
177 surface, which is expected since the O₂ oxidation reactions are assumed mass transfer limited, and O₂
178 is consumed in the boundary layer of the particle. Significant steam concentration gradients are
179 present inside the particle, emphasizing the conversion of char-C by steam. Also, relatively high
180 concentrations of CO₂ are present inside the particle, although the combustion occurs in an O₂/H₂O/N₂
181 mixture. This can be explained by the fact that steam reacts with char, producing H₂ and CO. In the
182 boundary layer of the particle the CO reacts to CO₂, consuming O₂. The formed CO₂ can diffuse back to
183 the char particle and gasify the char carbon. Thus, also CO₂ contributes to the consumption of char-C.

184 Park et al. [12] suggested that CO_2 reacts with char-N of coal to form N_2 . This reaction has to the
185 authors' knowledge not been investigated for biomass chars and is out of the scope of the present
186 study.

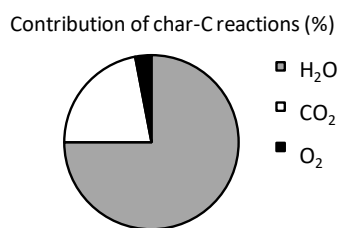
187 Figure 7 shows the relative contribution of H_2O , CO_2 and O_2 on the conversion of char-C. These
188 computations show that 75% of the char-C has been consumed by H_2O , 22% by CO_2 and only 3% by O_2 .
189 Similar calculations have previously been done for char-C of coal under pulverized fuel combustion
190 conditions [30]. The results of the present study imply that the most of char-C consumption is due to
191 steam gasification. Thus, by assuming that the conversion of carbon and nitrogen is non-selective; the
192 dominant species for converting the char-N in $\text{O}_2/\text{H}_2\text{O}/\text{N}_2$ is steam. It should be noted that it is possible
193 that also CO_2 influence the conversion of char-N. In Fig. 6 it can be seen that the concentration of H_2
194 is significantly lower than of CO inside the particle. This can be explained by the fact that the diffusion
195 coefficient of H_2 is significantly higher than of CO in the gas mixture. In the simulations, only one
196 particle size was considered. It can be expected that as the particle size decreases, the relative role of
197 oxygen increases, while the relative roles of CO_2 and steam on the char conversion decrease. For so
198 low temperatures and small particle sizes, that only O_2 , and not H_2O and CO_2 , would oxidize the char
199 it is plausible that H_2O would not influence the conversion of char-N to NO .



200

201 Fig. 6. Concentration profiles of H_2O , H_2 , CO , CO_2 and O_2 during single particle char combustion in
202 a mixture with 3% O_2 and 14% H_2O at 900 °C.

203



204

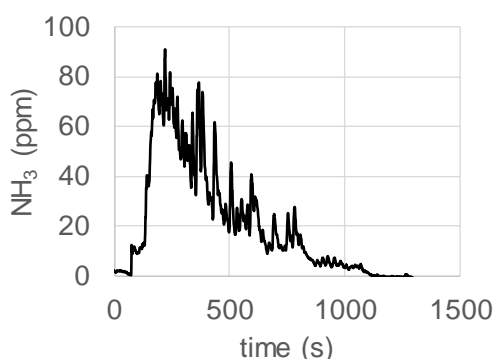
205 Fig. 7. Relative role of char-C oxidation by H₂O, CO₂ and O₂ during single particle char combustion
 206 in a mixture with 3% O₂ and 14% H₂O at 900 °C.

207

208 **3.3 Heterogeneous chemistry: formation of NH₃**

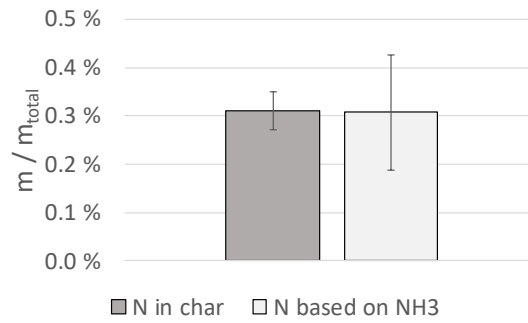
209 Fixed bed experiments were conducted to investigate the influence of steam on char-N. Figure 8 shows
 210 measured NH₃ concentration in product gases from steam gasification experiments of bark char. It can
 211 be seen that significant amounts of NH₃ are detected in the product gases experiments. The data
 212 shown is unfiltered explaining the noise. By integrating the measured concentrations of NH₃ and based
 213 on the total gas flow, the amounts of N were determined.

214 Fig. 9 shows the nitrogen contents of the char as determined from elemental analysis and as
 215 determined from NH₃ measurements based on five repeated steam gasification tests. The average N
 216 content, based on the NH₃ corresponds well to the elemental N content, implying that the char-N
 217 reacts entirely to NH₃. For coal chars it has been suggested that around 50% of the char-N forms NH₃
 218 under steam gasification [12].



219

220 Fig. 8. NH₃ as a function of time from fixed bed steam gasification of biomass char at 900 C with 3%
 221 H₂O in the gas.



222

223

Fig. 9. N contents of char based on elemental analysis and based on measured NH₃ concentrations

224

from fixed bed steam gasification experiments at 900 °C.

225

226

3.4 Homogeneous chemistry: oxidation of NH₃ to NO

227

The results of Fig. 8 and Fig. 9 show that NH₃ is the main reaction product from steam gasification of

228

the investigated biomass char. It may be expected that HCN, which was not measured, is also a reaction

229

product. To investigate the influence of NH₃ on NO formation in the combustion tests, the following

230

was done to model the homogeneous reactions of the flue gas: a detailed kinetic mechanism,

231

comprising 353 reactions, was used to compute conversion of NH₃ to NO [31]. The following was

232

assumed in the modeling: (1) an isothermal plug flow reactor with a temperature of 900 °C; (2) a gas

233

mixture with initial concentrations of 13.5% H₂O, 0.5% H₂, 0.5% CO, 2.5% O₂ and 5 ppm NH₃, with N₂ as

234

the balance gas. The initial concentrations were selected in the following way: the NH₃ concentration

235

was selected based on a typical value of the measured NO concentration in the single particle tests;

236

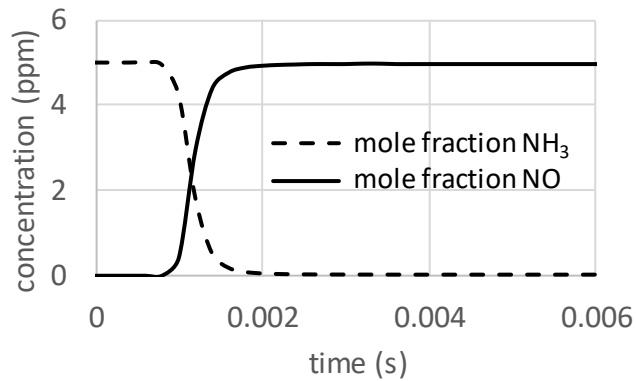
the CO concentration was selected based on a typical value of the measured CO₂ concentration in the

237

single particle tests; and the H₂ concentration was assumed to be the same as the CO concentration

238

which can be justified by that the steam gasification reaction $\text{H}_2\text{O} + \text{C}(\text{s}) \rightarrow \text{CO} + \text{H}_2$.



239

240 Fig. 10. Conversion of NH₃ to NO using detailed N chemistry mechanism isothermally at 900 °C,
 241 assuming the following initial concentrations: 13.5% H₂O, 0.5% H₂, 0.5% CO, 2.5% O₂ and 5 ppm
 242 NH₃.

243 Figure 10 plots the conversion of NH₃ to NO using the detailed N chemistry mechanism. Under the
 244 investigated conditions, the NH₃ reacts entirely to NO in less than 0.002s. The residence time in the
 245 single particle reactor, from the particle to the outlet of the reactor (this section of the reactor is
 246 heated), is around 1s, thus, several magnitudes higher than the time needed to oxidize NH₃ to NO
 247 based on the detailed kinetic mechanism. The kinetic simulations were repeated with initial values of
 248 NO between 0 and 2ppm, H₂ between 0 and 0.5%, CO between 0 and 0.5%, and CO₂ between 0 and
 249 0.2%. In each of these simulations, the NH₃ reacts entirely to NO. Note that these simulations were
 250 done to investigate the extent to which NH₃ reacts to NO in the single particle tests of the present
 251 study. These simulations imply that NH₃ reacts entirely to NO under the investigated conditions. In
 252 industrial thermal conversion systems, NH₃ is used to reduce the NO to N₂. Such a reduction is not
 253 occurring for the given gas mixture due to the low levels of NH₃ and NO.

254 3.5 Influence of steam on NO release

255 One explanation for the higher formation of NO during char combustion in H₂O/O₂/N₂ than in O₂/N₂ is
 256 that steam influences the conversion of char-N. The char-N reacts to NH₃, which reacts to NO. If NO is
 257 formed sufficiently far outside the char particle surface, then the NO cannot be reduced inside the
 258 pore structure of the particle. Since little O₂ reaches the particle surface, it is plausible that the
 259 oxidation of NH₃ occurs outside the char particle. On the other hand, when steam is not present in the

260 reactant gas, the char-N reacts with O₂ to NO, which can partly be reduced to N₂ inside the pore
261 structure of the particle. Thus, with steam present in the reactant gas, the final conversion of char-N
262 to NO is higher.

263 **3.6 Implications**

264 Previous studies have suggested that most NO_x emissions results from fuel-N released to NO_x
265 precursors during the devolatilization stage (e.g. [2,13]). While this conclusion may be valid, it is likely
266 in some cases that also the conversion of char-N influence the NO_x emissions. The results of the
267 present study show that the NO formation during the char combustion stage differs dependent on
268 whether there is steam present or not. In every combustion and gasification system, steam is present
269 to some extent. Thus, when investigating the NO formation during devolatilization and char
270 combustion, the influence of steam should be taken into consideration.

271 Little information is available in the literature regarding the behavior of fuel-N in industrial-scale
272 systems. Vainio et al. [32] conducted an experimental measurement campaign in a 107 MWth bubbling
273 fluidized bed firing bark. They measured NO, NH₃ and HCN in various vertical positions of the reactor.
274 One of the measurement points was 2m above the bed. They found that, in that height of the reactor,
275 the nitrogen present as NO, NH₃ and HCN corresponded to 96% of the fuel-N. The observed NH₃
276 concentrations were very high, i.e., almost 70% of the fuel-N had reacted to NH₃, strongly influencing
277 the final NO_x emissions. In this position almost no O₂ could be observed, suggesting that all O₂ of the
278 primary air through the bed had been consumed. In addition, relatively low concentrations of CO₂ were
279 observed in this position. On the other hand, the steam concentration of the gas was approximately
280 30%. This can be explained by the bark which had a very high moisture content of 60 wt.%. With such
281 a high steam concentration in the flue gas, it is possible that the char was gasified by steam, to a
282 significant extent, and that also the char-N reacted with steam to NH₃, based on the results of the
283 present study. This may help to explain why the NH₃ concentration in the primary combustion zone of
284 the fluidized bed was so high. In addition, if steam gasification reactions influenced the conversion of

285 char-N in the fluidized bed described above, then also the moisture content of the fuel influenced the
286 nitrogen release, since the cause for the high steam concentration in the primary combustion zone
287 was the high moisture content of the fuel. More work needs to be done on whether the fuel moisture
288 content can have an influence on NO_x emissions in combustion and gasification.

289 **4. Conclusions**

290 The following conclusions can be drawn from the present study:

- 291 • Char-N of the investigated biomass reacted with steam forming NH₃, while NO was not
292 observed as a reaction product.
- 293 • In single char particle experiments, significantly more NO was formed in mixtures of H₂O/O₂/N₂
294 than in O₂/N₂. This can be explained by the following: (1) in O₂/N₂, char-N forms NO, which is
295 partly reduced inside the pore structure to N₂; (2) in H₂O/O₂/N₂, char-N reacts partly with H₂O
296 to NH₃. This NH₃ oxidizes to NO outside the char particle and cannot be reduced by the char
297 surface, resulting in higher NO release. Thus, the heterogeneous NO reduction step is
298 eliminated in the presence of H₂O. These results were supported by results from single particle
299 modeling and chemical kinetics modeling of the homogeneous chemistry.

300 **Acknowledgement**

301 This study was financed by the Academy of Finland financed project with no. 289666 – Fate of
302 Fuel Bound Nitrogen in Biomass Gasification. The staff at Technical University of Denmark is
303 greatly acknowledged.

304 **References**

- 305 [1] Glarborg P, Jensen AD, Johnsson JE. Fuel nitrogen conversion in solid fuel systems. Progress Energy
306 Combust Sci 2003;29:89–113.
- 307 [2] Konttinen J, Kallio S, Hupa M, Winter F. NO formation tendency characterization for solid fuels in
308 fluidized beds. Fuel 2013;108:238–46.

309 [3] Lane D J, Ashman P J, Zevenhoven M, Hupa M, van Eyk P J, de Nys R, Karlström O, D. M. Lewis.
310 Combustion Behavior of Algal Biomass: Carbon Release, Nitrogen Release, and Char Reactivity. Energy
311 Fuels 2014;28:41–51.

312 [4] Hupa M, Karlström O, Vaino E. Biomass combustion technology development –It is all about
313 chemical details. Proceedings Combust Institute 2017; 36: 113–134.

314 [5] Vähä-Savo N. Behavior of black liquor nitrogen in combustion: formation of cyanate. Doctoral
315 thesis. Åbo Akademi University 2014.

316 [6] Yu QZ, Brage C, Chen GX, Sjöström K. The fate of fuel-nitrogen during gasification of biomass in a
317 pressurised fluidised bed gasifier. Fuel 86 (2007) 611–618.

318 [7] Song YH, Beer JM, Sarofim AF. Oxidation and devolatilization of nitrogen in coal char. Combust Sci
319 Techn 1982; 28: 177–183.

320 [8] De Soete GG. Heterogenous N₂O and NO formation from bound nitrogen atoms during coal char
321 combustion. Proceedings Combust Institute 1990;23:1257–1264.

322 [9] Karlström O, Brink A, Hupa M. Biomass char nitrogen oxidation - single particle model. Energy Fuels
323 2013;27:1410–1418.

324 [10] Karlström O, Brink A, Hupa M. Time dependent production of NO from combustion of large
325 biomass char particles. Fuel 2012; 103:524–532.

326 [11] Saastamoinen JJ, Taipale R. NO_x formation in grate combustion of wood. Clean Air 2003;4:239–
327 67.

328 [12] Park DC, Day SJ, Nelson PF. Nitrogen release during reaction of coal char with O₂, CO₂ and H₂O.
329 Proceedings combust institute 2005;30:2169–2175.

330 [13] Winter F, Wartha C, Hofbauer H. NO and N₂O formation during combustion of wood straw, malt
331 waste and peat. Bioresource Techn 1999; 70: 39–49.

332 [14] Ren Q, Zhao C. NO_x and N₂O precursors (NH₃ and HCN) from biomass pyrolysis: interactions
333 between amino acid and mineral matter. Applied Energy 2013; 112: 170–174.

334 [15] Toftegaard MB, Brix J, Jensen PA, Glarborg P, Jensen AD. Oxy-fuel combustion of solid fuels.
335 Progress Energy Combust Sci 2010; 36: 581–625.

336 [16] Hecht ES, Shaddix CR. Geier M, Molina A, Haynes BS. Effects of CO₂ and steam gasification
337 reactions on the oxy-combustion of pulverized coal char. Combust Flame 2012; 159: 3437–3447.

338 [17] Gómez-Barea A, Leckner B. Modeling of biomass gasification in fluidized bed. Progress Energy
339 Combust Sci 2010; 36: 444–509.

340 [18] Giuntoli J, de Jong W, Verkooijen AH, Piotrowska P, Zevenhoven M, Hupa M. Combustion
341 characteristics of biomass residues and biowastes: fate of fuel nitrogen. Energy Fuels 24; 2010: 5309–
342 5319.

343 [19] Karlström O, Perander M, DeMartini N, Brink A, Hupa M. Role of ash on the NO formation during
344 char oxidation of biomass. Fuel 2017;190:274–280.

345 [20] Zhao K, Glarborg P, Jensen AD. NO Reduction over Biomass and Coal Char during Simultaneous
346 Combustion. Energy Fuels 2013;27:7817–7826.

347 [21] Zhang Y, Ashizawa M, Kajitani S, Miura K. Proposal of a semi-empirical kinetic model to reconcile
348 with gasification reactivity profiles of biomass chars. Fuel 2008;87:475–481.

349 [22] Dupont C, Jacob S, Marrakchy KO, Hognon C, Grateau M, Labalette F, Da Silva Perez D. How
350 inorganic elements of biomass influence char steam gasification kinetics. Energy 2016; 109: 430–435.

351 [23] Zheng Y, Jensen AD, Glarborg P, Sendt K, Haynes BS. Heterogeneous fixation of N₂: investigation
352 of a novel mechanism for formation of NO. Proceedings Combust Inst 2009;32:1973–80.

353 [24] A. Molina, E. G. Eddings, D. W. Pershing, A. F. Sarofim. Char nitrogen conversion: implications to
354 emissions from coal-fired utility boilers. Progress Energy Combust Sci 2000;26:507–531.

355 [25] J. M. Jones, P. M. Patterson, M. Pourkashanian, A. Williams. Approaches to modelling
356 heterogeneous char NO formation/destruction during pulverised coal combustion. Carbon
357 1999;37:1545–1552.

358 [26] P. J. Ashman, B. S. Haynes, A. N. Buckley, P. F. Nelson. The fate of char-nitrogen in low temperature
359 oxidation. Proceedings Combust Institute 1998;27:3069–3075.

- 360 [27] L. L. Baxter, R. E. Mitchell, T. H. Fletcher, R. H. Hurt. Nitrogen release during coal
361 combustion. *Energy Fuels* 1996;10:188–196.
- 362 [28] B.R. Stanmore, S.P. Visona. *Combust Flame* 1998;113:274–276.
- 363 [29] O. Karlström, A. Brink, M. Hupa. *Combust flame* 2015;162:788–796.
- 364 [30] E. S. Hecht, C. R. Shaddix, A. Molina, B. S. Haynes. *Proceedings Combust Institute* 2011;33:1699–
365 1706.
- 366 [31] Coda Zabetta, E., Hupa, M., A Detailed Kinetic Mechanism with Methanol for Simulating Biomass
367 Combustion and N-Pollutants. *Combust Flame* 2008;152:14–27.
- 368 [32] Vainio E., Brink A, Hupa M, Vesala H, Kajolinna T. Fate of Fuel Nitrogen in the Furnace of an
369 Industrial Bubbling Fluidized Bed Boiler during Combustion of Biomass Fuel Mixtures. *Energy Fuels*
370 2012;26:94–101.